Tampere University

Otto Linros

NOVEL YTTERBIUM DOPED GLASS CERAMICS FOR FIBER LASERS

Effect of Al-, Ti- and Zn-oxides on the optical and luminescence properties and water absorption resistance

Bachelor Thesis
Faculty of Engineering and Natural Sciences
Prof. : Laeticia Petit
MSc. : Mikko Hongisto
April 2021

ABSTRACT

Otto Linros: Novel ytterbium doped glass ceramics for fiber lasers
Bachelor Thesis
Tampere University
Science and Engineering
April 2021

Phosphate laser glasses and glass ceramics are versatile materials, whose potential as a fiber laser core material has been studied. Often the lasing properties of a phosphate glass ceramic is not sufficient for laser applications, partly because the high water concentrations of phosphate glasses and glass ceramics lower the optical and luminescence powers of the material. Therefore, the goal of this study was to develop a new ytterbium doped oxyphosphate glass system with enhanced water resistance and lasing properties, and to study its compatibility to prepare a glass-ceramic, ultimately to be used in fiber laser glass cores.

An existing glass composition of (98.75) [(90)$NaPO_3$ – (10)Na_2O] – (1.25)Yb_2O_3 was modified by adding metal oxides into it, with the aim to enhance its water resistance and lasing properties. The added metal oxides were chosen to be Al_2O_3, TiO_2 and ZnO. The prepared glasses were also heat-treated into glass ceramics. The absorption coefficients and absorption cross-sections at approximately 975 nm were measured to evaluate the optical properties, and emission intensities and emission cross-sections were measured to evaluate the luminescence properties. The IR-spectra of the glasses were measured to check the presence of water in the glasses. Thermal analysis (DSC) and density measurements were conducted to evaluate the thermal and physical properties of the glasses. Also, the heat-treated glasses were studied with an XRD, to analyze their crystalline structure and composition.

The addition of Al_2O_3 and TiO_2 leads to an increase in the measured thermal properties, while the addition of ZnO showed no impact on the thermal properties. Addition of all the oxides showed an increase on the optical and luminescence properties, and a clear decrease on the water content of the glasses. Heat-treatment leads to the growth of a crystalline phase of $NaYb(P_2O_7)$ in all the glasses. Overall, the new glass compositions appear to be more water resistant than the base glass. The new glasses have increased optical and luminescence properties, and show a promise to be turned into optically active glass ceramics, possibly to be further used in fiber lasers.

Further research should be done on the long-term water absorption of these and similar glasses. The heat-treatment of the glasses should also be further optimized to achieve transparent glass ceramic, rich with Yb^{3+} containing crystalline phases in the bulk. Additionally, similar research needs to be done with different metal oxides, for example MgO and Li_2O which have been shown to be promising in other studies, to determine the best candidate for fiber laser applications.

Keywords: phosphate glasses, ytterbium laser glasses, glass ceramics, fiber laser, luminescence

CONTENTS

LIST OF SYMBOLS AND ABBREVIATIONS

Δ E	Activation energy
ΔG	Free energy of crystallization
ΔW	Net free energy change
$\Delta\lambda_{eff}$	Fluorecence effective linewidth
α	Absorption coefficient
$\bar{M}_g$	Average molar mass of a glass
λ	Wavelength
μ	Attenuation coefficient
ν	Atomic vibration frequency
ρ	Density
σ_{abs}	Absorption cross section
σ_{em}	Stimulated emission cross section
θ	Angle
A	Spontaneous emission probability
$\mathbf{a}$	Acceleration
c	Speed of light
d	Distance
DSC	Differential scanning calorimeter
E	Energy
f	Frequency
F_b	Buoyant force
FTIR	Fourier transformation infrared
g	Standard acceleration of free fall
h	Plancks constant
I(λ)	Intensity of emission
I(T)	Nucleation rate
J	Total momentum

l	Sample thickness
M	Molar mass
m	Mass
N	Number of atoms
n	Number density of atoms
N_A	Avogadro's number
R	Gas constant
T	Temperature
T_λ	Transmittance
T_g	Glass transition temperature
T_L	Littleton softening point
T_m	Glass melting temperature
T_n	Peak nucleation temperature
T_p	Peak crystallization temperature
T_x	Onset point
U(T)	Crystal growth rate
V	Volume
x_{Yb}	Molar fraction of Yb_2O_3
XRD	X-ray diffraction

1 INTRODUCTION TO THE STUDY

Photonics is the science of light and thus it studies the generation, the manipulation, and the detection of photons. Photonics research has been heavily dependent on lasers and laser technology since their discovery in the early 1960s [1]. Lasers are defined by the radiation they emit which is coherent and monochromatic light. This kind of light can be focused and directed with relative ease using different kinds of mirrors, filters, and glasses and therefore lasers are excellent for measuring wavelength dependent properties of materials such as absorption. Laser technology has progressed very quickly on the past few decades and at the moment the most powerful lasers, pulse lasers, can reach intensities as high as 10 petawatts with pulse length at the order of femtoseconds [1].

The other key element in photonics is glass. Optical glass is a very versatile medium and it is excellent at manipulating the direction of light and the frequencies of polychromatic light. Glasses can be further doped with optically active ions to turn them into laser glasses. Many base glasses like silicate and phosphate glasses have similar properties, yet also some differences. Most noticeable differences are in their durabilities and chemical stabilities. The most used glass, silicate glass, has a great chemical and physical durability, yet due to the low solubility of rare-earth ions, it is quite hard to dope with optically active ions [2]. Phosphate glass on the other hand suffers from poor water and chemical resistance but can be doped with higher amounts of optically active ions and other glass modifiers. Phosphate glasses have been extensively researched for many different optical applications and even in medical applications, such as synthetic bone transplants [3].

Recently, the Photonic Glasses group at Tampere University developed new transparent Yb^{3+} doped phosphate glass-ceramics in the $NaPO_3$-Na_2O glass system [4]. The heat treatment of the glass was found to lead to surface and bulk crystallization of $NaPO_3$, $Na_5P_3O_{10}$ and $NaYbP_2O_7$. However, the glass with composition of (90) $NaPO_3$ - (10) Na_2O was reported to be very hygroscopic, limiting its use. Hygroscopicity is a very unwanted property for glasses especially in optical applications, as water in glasses causes luminescence quenching of the optically active ion of Yb^{3+}. Furthermore, luminescence quenching causes noticeable losses in the intensity of the output radiation of the laser glass [5].

In this study, it is examined if the glass with composition of (90) $NaPO_3$ - (10) Na_2O can be tailored to be less water absorbing without changing the nucleation and growth process. Al_2O_3, TiO_2 and ZnO were chosen as the tuning agents to be added to the glass composition. This work was focused on the preparation and characterization of these new glasses in order to understand the relationship between glass composition, glass structure, optical properties, hygroscopicity, and nucleation and crystal growth.

2 THEORY OF GLASSES, LASERS AND GLASS CERAMICS

2.1 Glasses

2.1.1 Glass fundamentals

Glasses are highly used materials distinguished by their trait to be transparent in the visible spectrum of light. For this reason, glasses have been used for over 4500 years in human societies [6]. The uses of glass have varied greatly during the last four millennia ranging from obsidian arrowheads to the thousands of windows embedded in all inhabitable buildings. More modern uses for glass include the surface structure of solar panels [7] and most importantly for this research, the transparent core inside fiber lasers.

Glass is defined as a non-crystalline amorphous solid that experiences glass transformation behavior and therefore has no strictly defined melting point [8]. Normal solids have a well defined melting temperature on which their crystalline structure breaks and the material's enthalpy abruptly grows to the level of the liquid state. On the contrary, glasses do not have well defined melting temperatures, and their enthalpy does not increase rapidly in any temperature. This is partly because glasses do not have an ordered crystalline structure, they have an amorphous structure which lacks long range order. Because of this, the glass network breaks gradually with temperature and the enthalpy of the glass also rises gradually when the glass turns more liquid. The temperature range on which the glass's enthalpy rises faster than linearly, and in which the glass "melts", is called the glass transformation range. A comparison of glass and crystalline material's enthalpy to temperature diagrams can be seen on Figure 2.1.

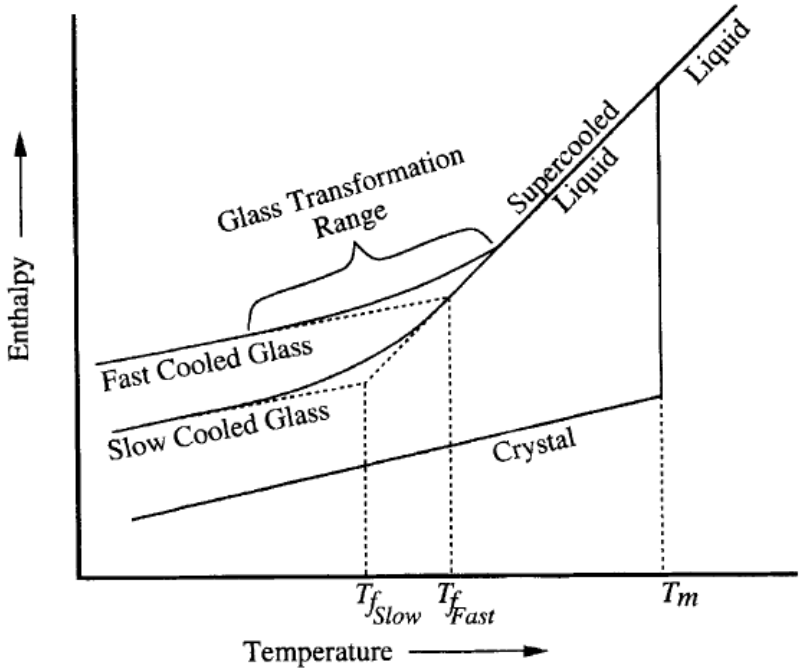

Figure 2.1. *Enthalpy as a function of temperature of a glass cooled with different rates and of crystallization of the same glass, Reproduced from [8].*

In addition to enthalpy, glasses can be viewed on how their viscosity changes with temperature. Although glasses do not have well defined melting temperatures, some meaningful temperatures can be determined from their viscosities. One notable temperature is the glass transition temperature T_g in which a glass enters the glass transformation range. In the glass transition temperature a glass has viscosity in the range of 10^{12}– $10^{12.5}$ Pa*s [9]. Other notable temperatures are the glass melting temperature T_m, in which the glass can be considered a liquid, and the Littleton softening point T_L, in which glass deforms greatly under its own weight. On the Littleton softening point a glass has viscosity of $10^{6.6}$ Pa*s and in the melting point a glass has viscosity of 1 - 10 Pa*s [9]. A visualization of glass viscosity to temperature change can be seen on Figure 2.2.

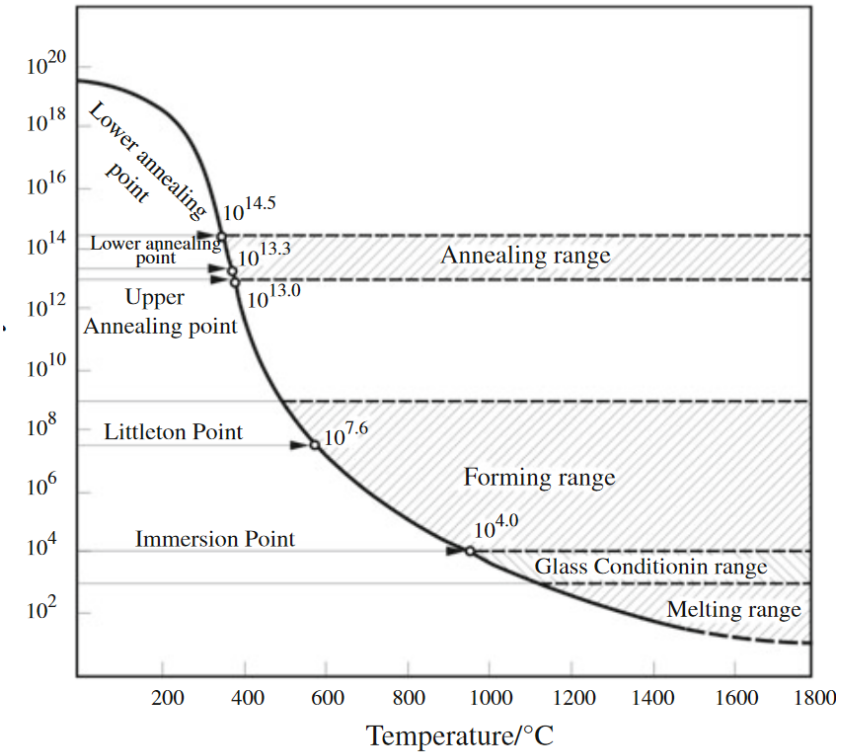

Figure 2.2. *Viscosity to temperature graph of a theoretical glass, Reproduced from [10].*

Structure of glasses can be described with the Zachariasen's Random Network Theory. It states the four rules of glass formation for an oxide of composition A_mO_n:

1. An oxide atom is linked to two cations A at the most.
2. The coordination number of the cation A is small.
3. The polyhedra formed around the cations A share only corners, not sides or edges.
4. For each polyhedra at least three corners are shared. [11] [12]

Oxides can be divided into three categories on their glass forming ability. **Network formers** are oxides which satisfy these rules and form glasses even by themselves, **network modifiers** are oxides which do not satisfy these rules and therefore do not form glass networks but only modify existing ones, and **intermediates** are oxides which sometimes form glass networks and sometimes act as modifiers. This division applies for almost all oxides, with only a few exceptions. Most typical network formers are SiO_4 and P_2O_5, typical network modifiers include CaO and Na_2O and examples of intermediates are Al_2O_3 and GeO_2 [8]. Additionally, some non-oxide substances like metals can act as network formers in the right circumstances [13].

2.1.2 Silicate and phosphate glasses

Silicate glass is the most widely used type of glass. It's glass network consists of silicon dioxide (SiO_2) tetrahedral units and some amounts of sodium and other ions in the case of soda-lime-silicate glass. The inner spatial structure of silicate glass is a genuine three-dimensional network of which the projected two-dimensional structure can be seen on Figure 2.3.

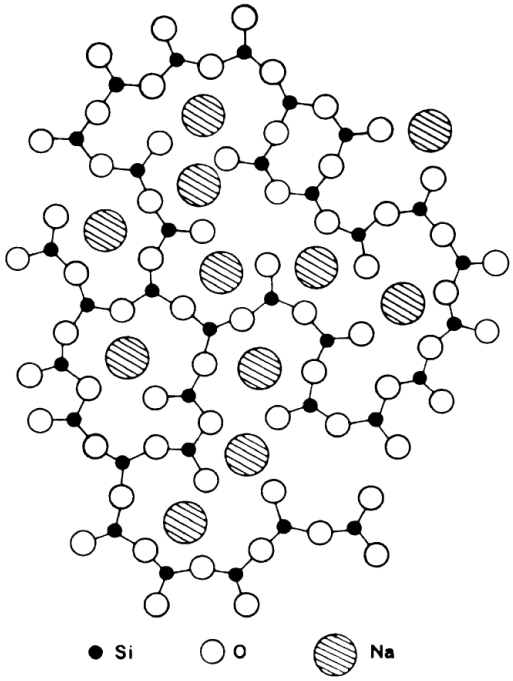

Figure 2.3. *Projected two-dimensional view of a silicate glass network, Reproduced from [14].*

Silicate glasses have very high melting temperatures, in the range of 1500 - 2000 ℃ depending on the composition of the glass [11] [15]. This is at the same time an asset and a liability. The higher melting temperature causes the glass to be more thermally durable, but also causes the melt to be more corrosive. High temperature melts can attack the crucible used for melting or react more readily with the atmosphere above the melt. However, rare-earth ion solubility is relatively low in silica/silicate glasses for their dense and strongly bonded silicate network [2].

Other common glass system used in optical applications is the phosphate system. Unlike silicate glasses, phosphate glasses can be manufactured at relatively low temperatures, at around 800-1300 ℃ [3], which makes them easier to produce in laboratory conditions. Phosphate glasses consist of interlinked orthophosphate (PO^{4-}_3)tetrahedra as the network former base unit which are connected to maximum of three neighboring other PO^{4-}_3 -molecules. Phosphate glasses are less dense, and this causes phosphate glasses to have higher rare-earth ion solubility than silicate glasses. [16] Phosphate glasses are

also soluble to water because of their structure. This low water resistance and the following high hygroscopicity are often seen as a liability in optical applications. Though in some applications, this is seen as an advantage. As an example, phosphate glasses have been studied for synthetic bone transplants for their low toxicity and high water solubility [3].

Phosphate glass's water resistance is dependent on the composition, but as a basic rule, the higher the concentrations of P_2O_5 and Na_2O in the glass, the lower the water resistance of the glass [17]. This is mostly due to water being attracted to the highly polar π-bonded oxygens in the phosphate chains. Also, the added sodium acts as a network modifier, which breaks the connectiveness of the phosphate network, and thus it is easier for outside water to enter the more porous glass matrix. [18] When water enters the phosphate glass network, it breaks the P-O-P -bonds into separate P-OH -bonds and thus lessens the connectiveness of the network [3]. Also, because the water is usually bonded in the glass structure as hydroxyl (OH^-)-groups, the water content of the glass is almost analogous to the hydroxyl-content, which is often the one being measured.

2.2 Laser glasses

2.2.1 Physics of lasers

Photons interact with atoms and molecules by scattering and absorption. Absorption occurs when an atom absorbs a photon, in which the photon vanishes and transfers its energy to an electron in the atom's outer electron shells. The electron moves to a higher energy level and becomes excited, and also its energy is increased by the amount of the photon's energy following the equation

$$E = hf, \tag{2.1}$$

in which h is the Planck constant and f is the frequency of the photon.

The electron can return to the original state radiatively through two different methods, the first is by **spontaneous emission** and the second is by **stimulated emission**. In **spontaneous emission** the excited electron returns from the excited state to its normal state and emits a photon whose energy matches the energy difference of the electron when it is in the excited state and when it is in the the ground state. The electron can also return to the ground state through multiple mid-states. Then the electron emits multiple photons consecutively with lower energies. When a material, like glass for example, experiences spontaneous emission and emits electromagnetic radiation, the process is called luminescence.

The second main phenomenon of emission is called **stimulated emission**. In stimulated

emission the electron in an excited energy level is influenced by a near passing photon of known frequency, polarization, and direction. This causes the excited electron to return to the ground state and emit a photon with same frequency, polarization, and direction as the original one, thus creating a copy of the original photon. Stimulated emission on a three energy level system is depicted in Figure 2.4.

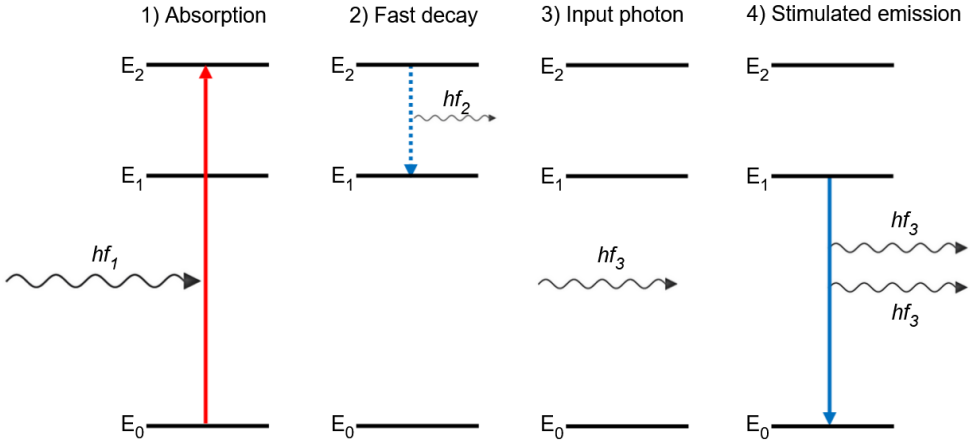

Figure 2.4. *Schematic of absorption and emission on a three energy level system.*

Lasers work on the basis of stimulated emission, and usually the gain medium, which is an ion or an atom, is a system of three or four energy levels. In the three energy level system a pump radiation source is used to excite the electron into a higher energy level 1, after which the electron rapidly and spontaneously falls into a lower energy level 2 emitting a lower energy photon. After this, photons with a known energy are guided into the excited electron, after which the electron degrades from the energy level 2 into the ground level amplifying the photon ray guided into it.

2.2.2 Rare-earth doped glasses

Laser glasses are glasses with rare-earth ions embedded in them. Rare-earth elements include all the elements in the lanthanoid series, and also scandium and yttrium. Rare-earth ions are the key ingredient of laser glasses because most of the optical phenomena, which include absorption, emission, and stimulated emission, occur on the electron shells of the rare-earth ions.

Laser glasses are commonly doped with erbium, yttrium, or ytterbium. Erbium doped laser glasses are based on the Er^{3+}-ion which can be pumped from energy level $^4I_{11/2}$ at wavelength of 980 nm, or from energy level $^4I_{13/2}$ at wavelength of 1480 nm, and the emitted photons are in the wavelength range of 1530- 1550 nm [19]. Because of the deep IR-emission of erbium laser glasses, they are highly used in the telecommunications sector. Yttrium on the other hand is often embedded in laser glasses as yttrium aluminum

garnet (YAG) crystals. YAGs are very promising laser glass gain materials for they experience wide emission bandwidths, high quantum efficiencies and low pump defects [20].

Ytterbium, the second to last element of the lanthanide series, is also often used in laser glasses. Ytterbium has two ionic forms Yb^{2+} and Yb^{3+}. The trivalent ion is the most chemically stable ionic form and under normal conditions it only has one possible energy transition from energy level $^2F_{5/2}$ to $^2F_{7/2}$. The energy difference on this transition corresponds with a photon that has a wavelength of approximately 960 nm. This energy transition is illustrated in Figure 2.5. The simplicity of the possible energy transitions makes Yb^{3+} ideal for laser applications because it experiences little heat-based losses and it has well-defined pumping wavelengths and wavelengths of emission.

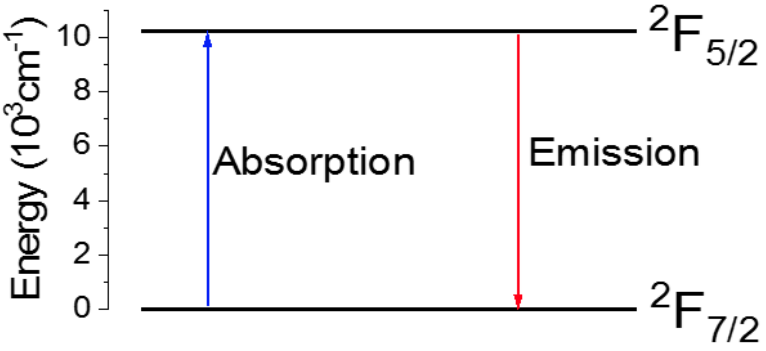

Figure 2.5. *Simplified energy levels of Yb^{3+}.*

Though when used as a gain medium for a laser glass, Yb^{3+}-ion experiences major losses in the emission efficiency due to hydroxyl quenching [5]. The bonded OH-groups in the glass structure partially absorb the source photons or the emitted photons from the Yb^{3+}-ions and turn the photons' energy into inner energy of the glass material, mainly into heat. This lowers the efficiencies of absorption and emission for the laser glass systems and therefore hydroxyl quenching is considered to be a major disadvantage in most optical phosphate glass systems. [21] The absorption and emission processes for the Yb^{3+}-ion are also very sensitive to changes in the coordination sphere of the ion, i.e. primarily and secondarily connected ligands around the Yb^{3+}-ion [22].

2.3 Glass ceramics

2.3.1 Nucleation and crystal growth

Glass can be turned into a glass ceramic, by growing small (10-1000 nm) crystals inside the bulk of the glass using heat-treatment. The heat-treatment process can be divided to two separate phases; in the first phase nucleation centers are created into glass, and in the second phase those nucleation centers are grown into crystals. The formation of

nuclei is called nucleation. The nucleation rate is defined as

$$I(T) = N\nu \exp\left(-\frac{N_A \Delta W}{RT}\right) \exp\left(-\frac{\Delta E_i}{RT}\right), \tag{2.2}$$

in which N is the number of atoms, ν is the atomic vibration frequency, N_A is Avogadro's number, ΔW is the net free energy change, R is the gas constant, T is the temperature and ΔE_i is the activation energy of interface change [11].

The second phase, which is the crystal growth phase, occurs in higher temperatures and grows the size of the already formed nuclei. Crystal growth rate is defined as

$$U(T) = d\nu \exp\left(-\frac{\Delta E_m}{RT}\right)\left[1 - \exp\left(\frac{\Delta G}{RT}\right)\right] \tag{2.3}$$

in which d is the distance between two growth sites, ΔE_m is the activation energy of motion and ΔG is the free energy of crystallization [11].

The heat-treatment process is done in accordance with the used glasses nucleation and crystal growth rates. These rates are unique for all glasses and need to be measured, but they always follow a certain pattern. When these rates are plotted as a function of temperature, they form two distinct bell-curves of which the temperature at the peak of the nucleation rate is denoted T_n and the temperature at the peak of the crystal growth rate is denoted T_p. A typical nucleation and crystal growth rate to temperature graph is presented in Figure 2.6.

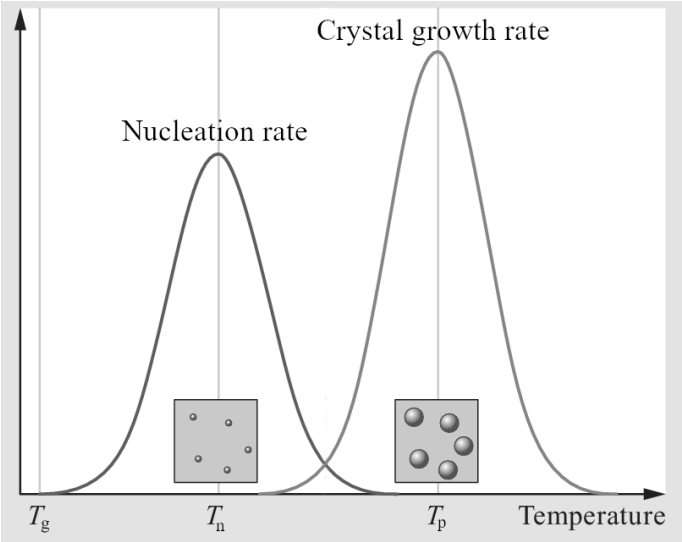

Figure 2.6. *Nucleation and crystal growth rates by temperature of a typical glass material, Adapted from [23].*

In this study the glasses were heat-treated into glass-ceramics. Firstly, the glasses were heated in a temperature where the nucleation rate I(T) is high, at temperatures between

T_g and T_n. Secondly, they were heated in a higher temperature where the crystal growth rate U(T) is as high as possible, around T_p. Though some glasses have a large temperature range in which the nucleation rate and crystal growth rate overlap. This can be troublesome if one wishes to get homogenously sized crystals in the glass, and then it might be necessary to do more extensive measurements for I(T) and U(T) to minimize the time the glass is in the temperature range on which the two rates overlap.

2.3.2 Yb^{3+} doped glasses

Yb^{3+}-doped glasses have been widely used in optical applications like lasers, for the simplicity of the ions energy levels. Yet it might be possible to further increase the optical properties of the Yb^{3+}-doped glasses by turning them into glass ceramics. This was studied by Hongisto et. al. on Yb^{3+}-doped oxyfluorophosphate glasses within the $NaPO_3$ – Na_2O – NaF -system. In their study they showed, that if the glass did not contain fluorine, it could be transformed into a transparent glass ceramic. Even though the Yb^{3+} doped glass with the (90) $NaPO_3$ - (10) Na_2O composition could be heat-treated into transparent glass-ceramic, this glass was too hygroscopic, limiting its use. [4] The goal of this study was to add network modifiers or intermediates to this fluorine free Yb^{3+}-doped oxyphosphate glass system, to increase the water resistance, and thus lower the hygroscopicity of the glass.

It was found that the fluorine free glass grew into at least three different crystalline phases which were $NaYbP_2O_7$, $Na_5P_3O_{10}$ and $NaPO_3$ [4]. Though for optical applications such as fiber lasers, the good crystalline phases should include the optically active rare-earth ion, as in this case is Yb^{3+}. Therefore, the only good crystalline phase from the ones listed above would be the $NaYbP_2O_7$ -phase. The $NaYbP_2O_7$ -phase is known to change the energy levels of Yb^{3+}-ion and thus change the emission and absorption processes of the glass [24]. Though, this change in the optical properties is sometimes even preferable, for the emission tend to move towards the IR-region which is highly used in, for example, telecommunication and laser applications.

3 MEASUREMENT AND ANALYSIS METHODS

3.1 Sample preparation

All the glasses were prepared with the composition of (98.75 - x) mol% [90 $NaPO_3$ – 10 Na_2O] – x mol% [Al_2O_3, TiO_2, or ZnO] – 1.25 mol% [Yb_2O_3] with x ranging from 0 to 6. The raw materials were Al_2O_3 -powder (Sigma-Aldrich, 99.997%), granular $(NaPO_3)_6$ (Alfa-Aesar, tech), Na_2CO_3 -powder (Sigma-Aldrich, 99.5%), TiO_2 -powder (Sigma-Aldrich, 99.8%), Yb_2O_3 -powder (Sigma-Aldrich, 99.9%) and ZnO -powder (Sigma-Aldrich, 99.99%).

The glasses were prepared using the standard melt-quench -method. The melting temperature varied between 1000 and 1100 ℃ depending on the glass composition. The glasses were melted in platinum crucible after which they were quenched on a brass plate and finally, they were annealed in 250 ℃ for five hours to relieve any internal stresses. After annealing, the glasses were heat treated at T_g + 20 ℃ for 17 hours and then at T_p for two hours.

3.2 Physical and thermal analysis

The thermal properties of the glasses were analyzed with a differential scanning calorimeter (DSC) in a platinum sample holder. DSC functions by measuring the heat flow of two crucibles, an empty reference crucible and the crucible with the actual sample, while keeping both at the same constantly growing temperature. Basic functionality of a DSC is illustrated in Figure 3.1.

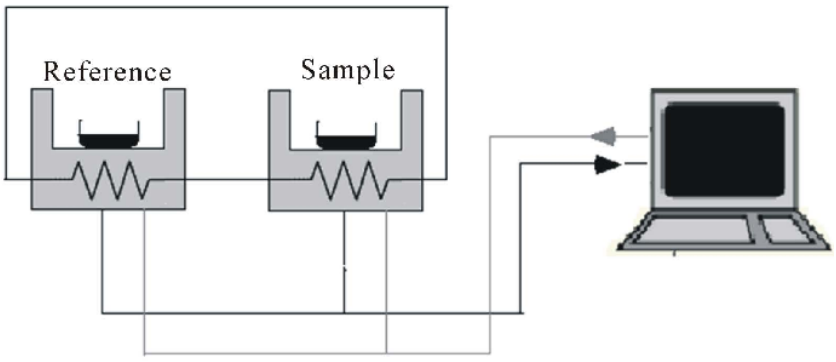

Figure 3.1. *DSC schematic graph, Reproduced from [25].*

A typical heat flow to temperature diagram for a glass is illustrated in Figure 3.2. The glass transition temperature T_g, the peak crystallization temperature T_p and the onset of crystallization T_x were determined from the DSC-graphs.

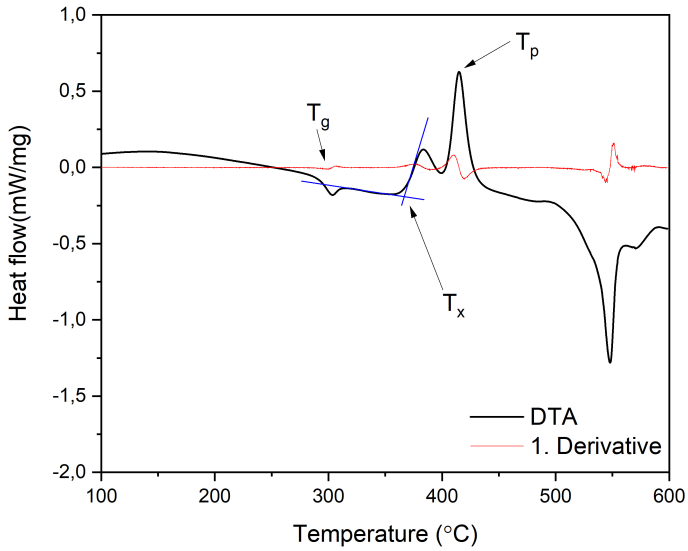

Figure 3.2. *Plotted DSC-figure of Zn-0.75%-glass with the corresponding temperatures as an example.*

T_g is the glass transition temperature, and it was determined by taking the first minimum of the derivative of the graph. T_p is the glass peak crystallization temperature, and it was determined as the maximum of the exothermic peak. T_x is the onset of crystallization. All measurements were performed with an accuracy of $\pm$ 3 ℃. Additionally an experimental quantity ΔT was determined as the temperature difference between T_g and T_x.

The densities of the glasses were measured using the Archimedes principle, which can be expressed as

$$F_b = V\rho g, \tag{3.1}$$

in which F_b is the buoyant force onto an object in an immersive fluid, V is the volume of the object, ρ is the density of the immersive fluid and g is the standard acceleration of freefall. With Equation 3.1 and Newtons first and second law in mind one can derive equation for the density of the glasses (or any other object)

$$\rho = \frac{\rho_e m_a}{m_a - m_e}, \tag{3.2}$$

in which ρ_e is the density of ethanol (the liquid used for the measurements), m_a is the mass

of the glass sample measured in air and m_e is the mass of the glass sample measured while immersed in ethanol. The accuracy of the measurements are $\pm$ 0.02 g/cm^3

The densities of the glasses were also used to calculate the number density of the Yb^{3+}-ions. The number density can be derived to the form

$$n = \frac{2N_A x_{Yb}}{\bar{M}_g}\rho, \tag{3.3}$$

where N_A is the Avogadro's constant, x_{Yb} is the molar fraction of Yb_2O_3 in the glass, $\bar{M}_g$ is the average molar mass of the glass and ρ is the density of the glass.

3.3 Optical properties

The transmittance of the glasses was measured with a Shimadzu UV-3600 Plus -spectrometer from 200 nm to 1700 nm. This data was used to further solve the absorption coefficients, and therefore to determine the effect of the glass composition on the absorbance. Absorption coefficient can be excluded from the attenuation coefficient, which is the summation of scattering, refraction, and absorption coefficients. Attenuation coefficient is defined as

$$\mu = \frac{ln(T_\lambda)}{l}, \tag{3.4}$$

in which T_λ is the measured transmittance and l is the sample thickness. The attenuation coefficient data was sufficiently normalized to get the absorption coefficient data of the glasses.

The calculated absorption coefficients were used to calculate absorption cross-sections for the glasses. Absorption cross-section is a measure that describes the probability of an absorption occurring in the outer electrons of a specific ion. Absorption cross-section is defined as

$$\sigma_{abs} = \frac{\alpha}{n}, \tag{3.5}$$

where α is the absorption coefficient and n is the number density of the ions [26]. The absorption cross-sections were calculated with an accuracy of $\pm$ 10 %.

3.4 Luminescence properties

The emission spectra of the glasses were measured with a fluorescence spectrometer with monochromatic excitation. The used spectrometer was FLS1000, Edinburgh Instrument spectrometer at excitation of 900 nm. The bulk sample measurements give the

wavelength dependent emission spectra of the glasses.

Another quantity related to emission is called stimulated emission cross-section. Stimulated emission cross-section describes the average probability of stimulated emission for the ions in the bulk material. Another interpretation of the stimulated emission cross-section is the average size of the area around the optically active molecule into which photons need to enter to initiate the stimulated emission. Using the concepts of spontaneous emission probability and effective fluorescence linewidth emission cross-section can be defined as

$$\sigma_{em} = \frac{\lambda^4 A}{8\pi c n^2 \Delta\lambda_{eff}}, \tag{3.6}$$

where A is the spontaneous emission probability and $\Delta\lambda_{eff}$ is the fluorescence effective linewidth [27] [26]. The spontaneous emission probability can be defined as

$$A = \frac{8\pi c n^2 (2J'+1)}{\lambda_p^4 (2J+1)} \int \alpha d\lambda, \tag{3.7}$$

in which J' and J are the total momentums for the upper and lower levels and λ_p is the absorption peak wavelength [27]. The fluorescence effective linewidth is defined as

$$\Delta\lambda_{eff} = \int \frac{I(\lambda)}{I_{max}} d\lambda, \tag{3.8}$$

in which I(λ) and I_{max} are the intensity and maximum intensity of emission [27]. The spontaneous emission cross sections were calculated with an accuracy of $\pm$ 10%.

3.5 Fourier transformation infrared -analysis

To analyze the water content of the prepared glasses Fourier transformation infrared (FTIR) analysis was used. The apparatus used was a Perkin Elmer FTIR Spectrum One with measurements done in range of 4500 cm^1 to 600 cm^1. FTIR spectroscopy setup is an application of the Michelson interferometer and its schematic diagram is depicted in Figure 3.3.

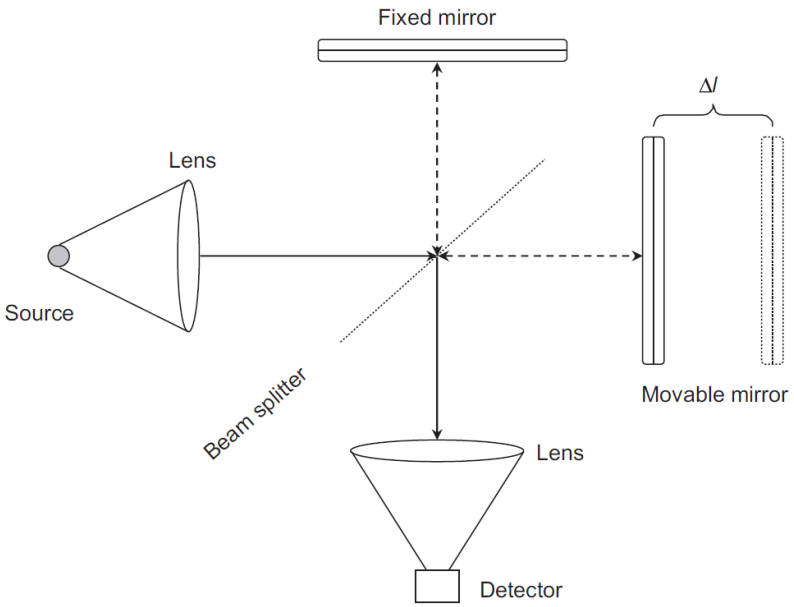

Figure 3.3. *FTIR Schematic diagram, Reproduced from [28].*

In FTIR measurements a beam of polychromatic light is guided through a Michelson interferometer mirror setup and through the sample to the detector as seen on Figure 3.3. The path length of one of the two divided beams is varied with the moving mirror and the intensity of the light hitting the detector is measured as a function of the path length change. The path length change causes constructive and destructive interference on the different wavelengths of the polychromatic beam. FTIR gets its name from the Fourier Transformation, which is used to transform the measured oscillating intensity by change of length data, into data of absorbed light intensity by wavenumber/wavelength of light.

3.6 X-ray diffraction -measurements

X-ray diffraction or XRD was used to determine the crystalline structure of the crystals precipitating in the glasses. A Malvern Panalytical Empyrean XRD was used at 40 kV and 45 mA excitation with Co-tube. XRD is based on a rotational apparatus that emits X-Ray radiation onto finely ground homogenous powder sample. The scattered radiation is then focused to a photosensor from which measures the relative intensity of the radiation. The basic structure of an XRD is shown in Figure 3.4.

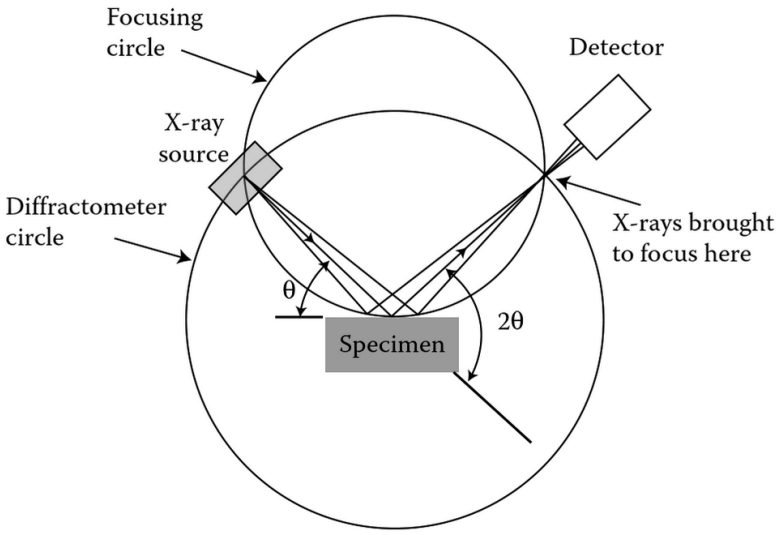

Figure 3.4. *XRD schematic graph, Reproduced from [29].*

XRD measurements are based on constructive interference of radiation in a crystalline lattice. The maximum constructive interference happens with angles fulfilling the Braggs condition

$$n\lambda = 2d\sin\theta, \tag{3.9}$$

in which n is a whole number, λ is the wavelength of the radiation, d is the distance between two arranged particles in the crystal lattice and θ is the angle between the sample surface and the beam. The measured intensity for certain angle θ is related to the number of lattices with particle distances d, and after measuring at larger angle scale one gets an overview of the average crystalline composition of the material.

To analyze the data from XRD-measurements one usually uses a database and an automatic search engine to match the measured sample and the correct crystalline phases. This is also what was done with this research and the used database was the *ICDD powder diffraction file*.

4 RESULTS AND OBSERVATIONS

4.1 Structure, optical properties and hygroscopicity of the glasses

The meaningful temperatures were measured, and the densities of the glasses were calculated and measured with Equation 3.2. The physical and thermal properties of the investigated glasses are gathered in Table 4.1.

	Al_2O_3					TiO_2					ZnO				
mol%	**0.0**	**0.75**	**1.5**	**3.0**	**6.0**	**0.0**	**0.75**	**1.5**	**3.0**	**6.0**	**0.0**	**0.75**	**1.5**	**3.0**	**6.0**
$\rho \pm$ **0.02 g/cm**^{3}	2.63	2.63	2.66	2.66	2.68	2.63	2.71	2.62	2.63	2.64	2.63	2.62	2.64	2.65	2.69
T_g **(°C)** $\pm$ **3 °C**	295	305	310	323	355	295	311	306	318	349	295	299	300	302	299
T_x **(°C)** $\pm$ **3 °C**	360	380	395	418	443	360	408	401	430	460	360	365	366	371	376
T_{p1} **(°C)** $\pm$ **3 °C**	375	397	412	433	464	375	424	421	453	486	375	383	384	394	391
T_{p2} **(°C** $\pm$ **3 °)**	397	442	476	492	512	397	447	487	-	587	397	415	425	435	506
Δ**T (°C)** $\pm$ **6 °C**	65	75	85	95	88	65	96	96	112	110	65	66	66	70	76

Table 4.1. *Thermal properties and densities of the glasses.*

As indicated on Table 4.1 the glass had a small increase in density with increase of aluminum. The transition temperature T_g, the onset of crystallization T_x, and the crystallization peak temperatures T_{p1} and T_{p2} of the glass also increase with aluminum. The density of the base glass had no significant change with the addition of TiO_2. Similar to the Al-glasses, the measured temperatures increased with the addition of TiO_2. Notably the empirical value of ΔT reached over 100 °C which is considered to be the minimum value for a glass to be a good fiber preform [3]. The density of the base glass experienced a slight increase with the addition of ZnO. The addition of ZnO had little to no effect on the measured temperatures of the glass. The empirical temperature value of ΔT was also clearly under the considered minimum value of 100 °C, and thus these zinc-glasses would not be well suited for fiber drawing [3].

The absorption of all the glasses were measured in the UV-vis -region and in the vis-IR -region. The measured absorption in the UV-vis -region are gathered in Figure 4.1. In the UV-vis -region the absorption edge can be detected and in the vis-IR -region the absorption peak of the Yb^{3+} can be detected, which is around the $^2F_{5/2}$ to $^2F_{7/2}$ energy level transition at approximately 975 nm. As seen from the graphs in Figure 4.1, the

absorption band gap of the Ti-glasses experiences a shift towards the visible range with increasing concentrations of the TiO_2. Also, slight shift can be detected on the Al-glasses, but not on the Zn-glasses.

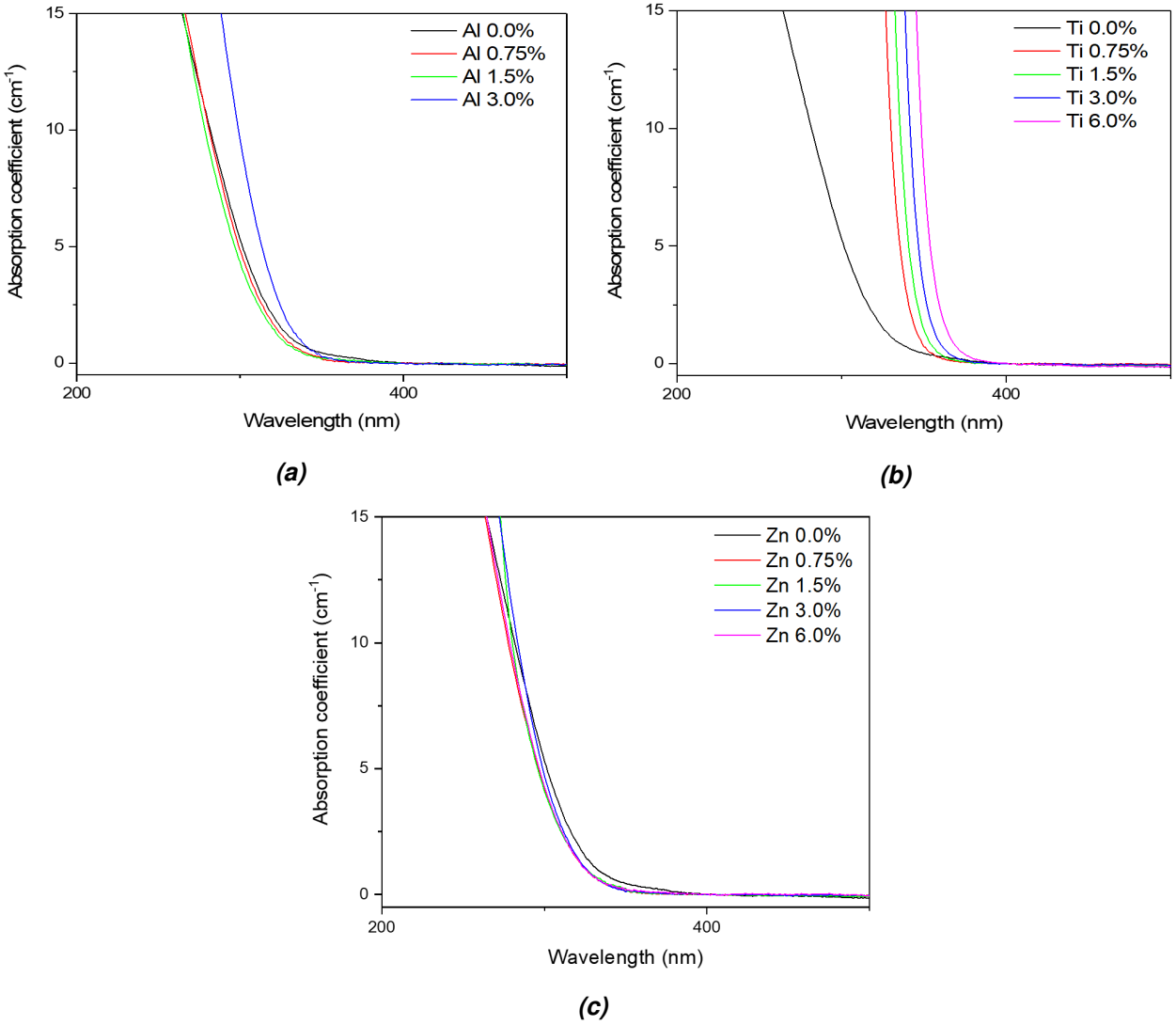

Figure 4.1. *Absorption bands of all the glasses in the UV-vis -range.*

The optical and luminescence properties of the glasses were measured and calculated, and they are gathered in Table 4.2. The number density of Yb^{3+}-ions in the glasses were calculated with Equation 3.3, the absorption coefficients of the glasses in the vis-IR-region were calculated with Equation 3.4, the absorption cross-sections were calculated with Equation 3.5 and the emission cross-sections were calculated with Equation 3.6.

	Al_2O_3					TiO_2					ZnO				
mol%	**0.0**	**0.75**	**1.5**	**3.0**	**6.0**	**0.0**	**0.75**	**1.5**	**3.0**	**6.0**	**0.0**	**0.75**	**1.5**	**3.0**	**6.0**
Yb^{3+} 10^{20} n·cm^{-3} ± 5%	3.91	3.92	3.98	3.97	3.99	3.91	4.03	3.92	3.94	3.98	3.91	3.93	3.94	3.96	4.06
α_{abs} **(cm^{-3})**	3.72	3.91	4.11	4.17	-	3.72	7.74	3.93	4.22	4.57	3.72	3.86	3.66	3.98	4.22
σ_{abs} **10^{-21} cm^2 ± 10%**	9.51	9.97	10.33	10.51	-	9.51	19.20	10.03	10.70	11.50	9.51	9.83	9.29	10.04	10.39
σ_{em} **10^{-21} cm^2 ± 10%**	4.32	4.88	5.28	5.33	-	4.32	7.37	5.05	4.98	5.58	4.32	4.28	4.13	4.56	5.13

Table 4.2. *Optical properties of the different glasses; the absorption coefficient α_{abs}, absorption cross-section σ_{abs} and emission cross-section σ_{em} are calculated at 975 nm.*

The addition of aluminum seems to increase the absorption coefficient and therefore also the absorption cross-section. These increases are an indication that the addition of Al_2O_3 changes the coordination sphere of the Yb^{3+} ion and thus changes the process and rate of energy transfer through absorption [30]. The addition of TiO_2 also appears to noticeably increase the values of the absorption coefficient and the absorption cross-section of the glass. The TiO_2 0.75 mol% -glass seems to be slightly of trend but this is probably due to manufacturing error of the specific glass batch. Similarly to the Al-glasses, it can be expected that the TiO_2 modifies the coordination sphere of the Yb^{3+} -ion and thus changes the absorption process and amplifies the absorption at the peak wavelength [30]. Just like with the addition of Al_2O_3 and TiO_2, the addition of ZnO also increases the absorption coefficient and absorption cross-sections, and for the same reason of modifying the coordination sphere of Yb^{3+}. The increase in the absorption coefficient implies that the addition of all the oxides increases the efficiency of energy transfer to the glass through absorption. The increase in absorption cross-section on the other hand indicates that the added oxides increase the pumping efficiency of the glass when the goal is to achieve high population inversion, such as in laser applications.

The changes in the thermal properties, density and in the optical properties are an indication that the glass structure changes with the addition of the Al_2O_3, TiO_2 and ZnO. The addition of Al_2O_3 and TiO_2 change the thermal properties, and as demonstrated by Metwalli et al. [31], it is expected that it is due to the formation of new P-O-Al/Ti bonds at the expense of P-O-P bonds. Also, the absorption measurements indicate the same results, for the Al- and Ti-glasses show a redshift of the absorption edge, which is an indication that new P-O-Ti and P-O-Al -bonds are created onto the glass network [32] [33]. As ZnO seems to have no impact on the thermal properties, ZnO is expected to enter the glass structure as a network modifier and therefore it does not affect the network structure of the glass. On the other hand, the increase of the absorption coefficient and absorption cross-sections in all the glasses indicates that the added oxides modify the coordination sphere of the optically active ion of Yb^{3+}.

The emission of the glasses were measured with a spectrometer at 900nm excitation to get the relative intensities of emission in different wavelengths. The measured emission spectra of the glasses were normalized to the highest peak at approximately 975 nm and they are gathered in Figure 4.2.

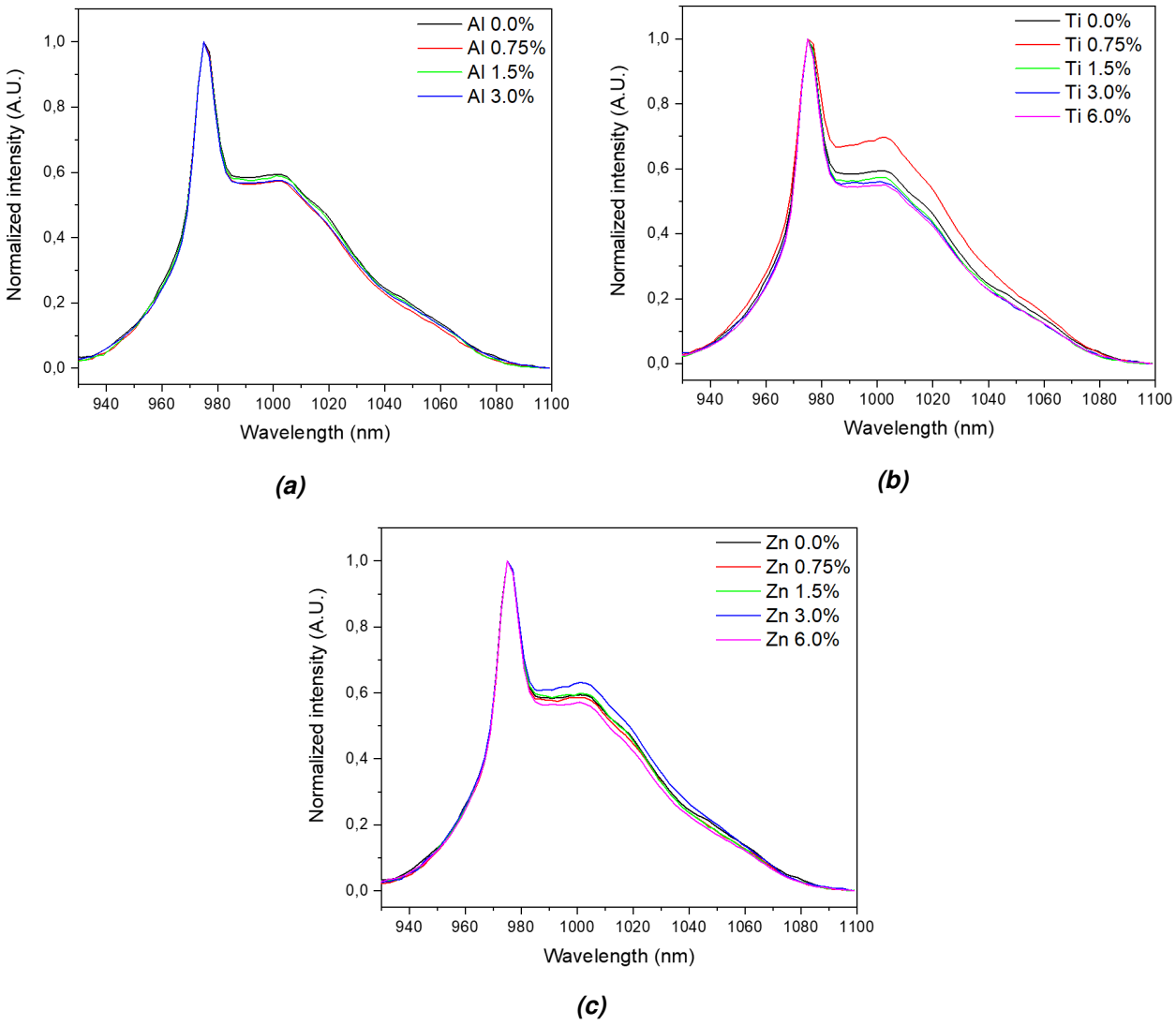

Figure 4.2. *Normalized emission spectra of the glasses with 900 nm excitation.*

In Figure 4.2 the emission intensities of all the glasses show an increase in the emission of the peak wavelength of 975 nm in comparison to the emission around 1000 nm – 1020 nm with increasing concentrations of the added ions. This indicates that the added oxides change the coordination sphere of the Yb^{3+} and cause an increase in the emission power [34].

In Table 4.2 the calculated emission cross-sections at 975 nm show a clear trend of increasing with the addition of all the added oxides Al_2O_3, TiO_2 and ZnO. This is also in line with the emission measurements and confirm that the coordination sphere of Yb^{3+} is

influenced, which causes an increase in the emission around the peak wavelength of 975 nm.

The measured FTIR-spectra of the glasses are shown in Figure 4.3. All the spectra are plotted around one major band at approximately 2800 cm^{-1} which corresponds with the inner OH-bonds which in turn are the result of absorbed water into the glass [35] [36].

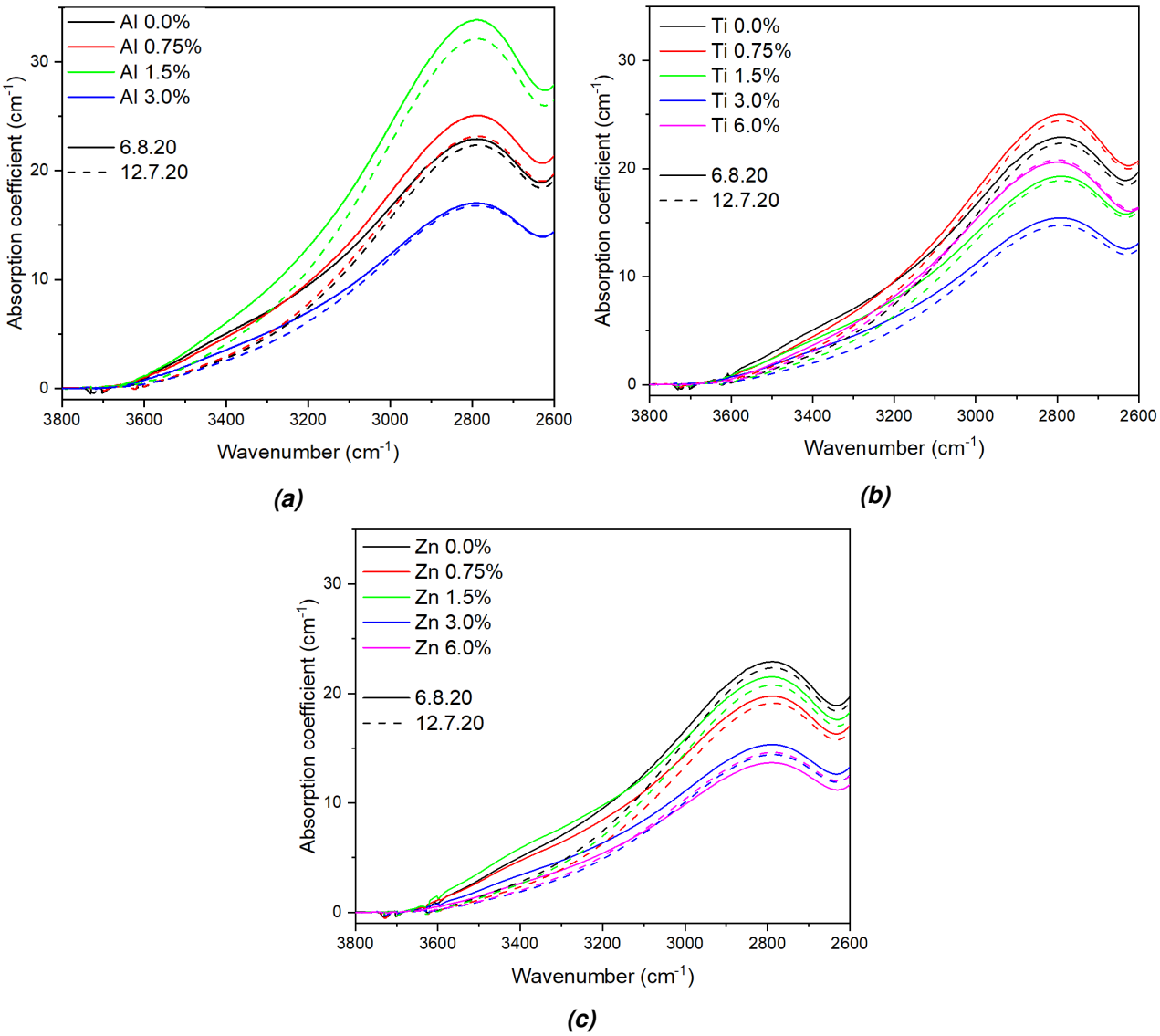

Figure 4.3. *IR-spectra of aluminum (a), titanium (b) and zinc (c) glasses.*

In the IR-spectra there is a clear decrease in intensity of the band centered at 2800 cm^{-1} with increasing concentrations of all the added oxides. The decrease of the intensity of this band indicates that the glasses contain less water with addition of the oxides. This further implies that the water resistance of the glass increases and hygroscopicity of the glass decreases with the addition of the oxides. Only the Al1.5% -glass had a considerably higher water content than the reference glass, but this is most likely due to manufacturing error. Also, for the 2800 cm^{-1} band increases over time, all the glasses demon-

strate some amounts of hygroscopicity, though this is typical for phosphate glasses.

4.2 Glass ceramics

After annealing, the glasses were heat treated at T_g + 20 ℃ for 17 hours and then at T_p for two hours. The heat-treated glasses turned opaque, as seen from Figure 4.4, and thus they were clearly crystallized.

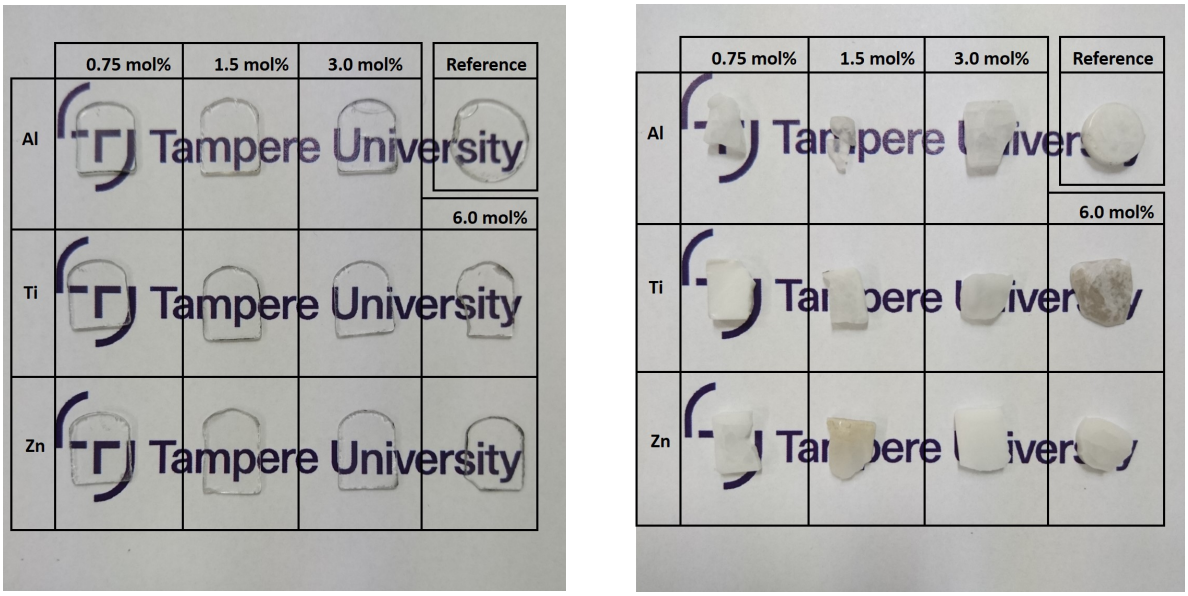

(a) ***(b)***

Figure 4.4. *Pictures of the glasses before (a) and after (b) heat treatment.*

The heat-treated glasses shown in Figure 4.4(b) were completely crystallized, so it is impossible to know if the crystals were formed mainly by surface crystallization or by bulk crystallization. For the use of fiber lasers, the preferable crystals would be bulk crystals homogenously distributed in the glass bulk.

The XRD-patterns of the heat-treated glasses were measured and can be seen on Figure 4.5. Also, the corresponding peak diagrams of the two found crystalline phases of $NaYb(P_2O_7)$ and $Na_5(P_3O_{10})$ are presented on the XRD graphs. The results indicate that all the heat-treated glasses had mainly these two crystalline phases and the amount or ratio of the crystalline phases did not change much by the addition of the oxides of Al_2O_3, TiO_2 and ZnO.

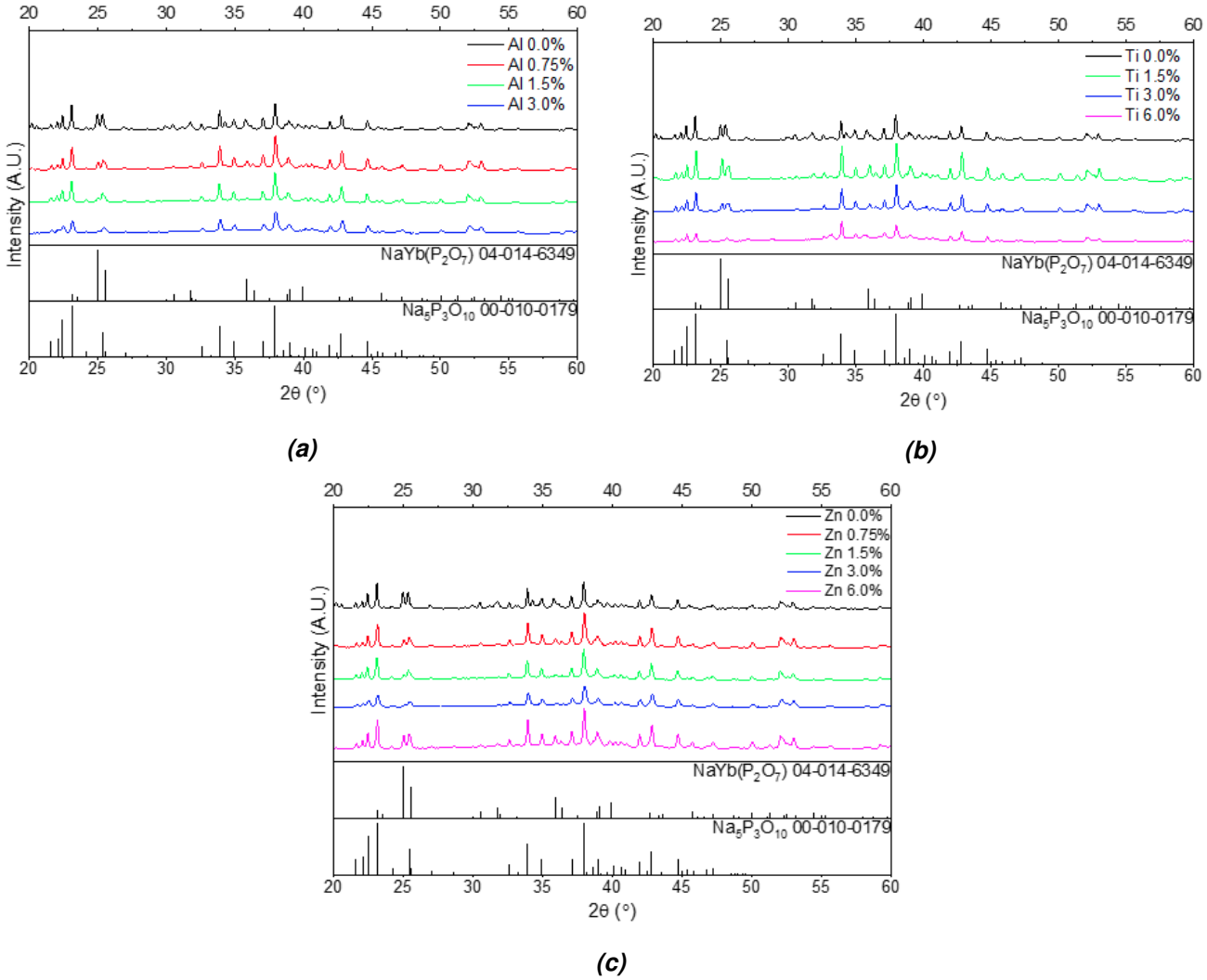

Figure 4.5. *XRD-patterns of Al- (a), Ti- (b) and Zn-glasses (c) after heat treatment.*

The relative emission spectra were measured for the heat-treated glasses with spectrometer at 900 nm excitation with the same setup as for the untreated glasses. The emission spectra were normalized around the highest peak at approximately 1005 nm and they can be seen on Figure 4.6.

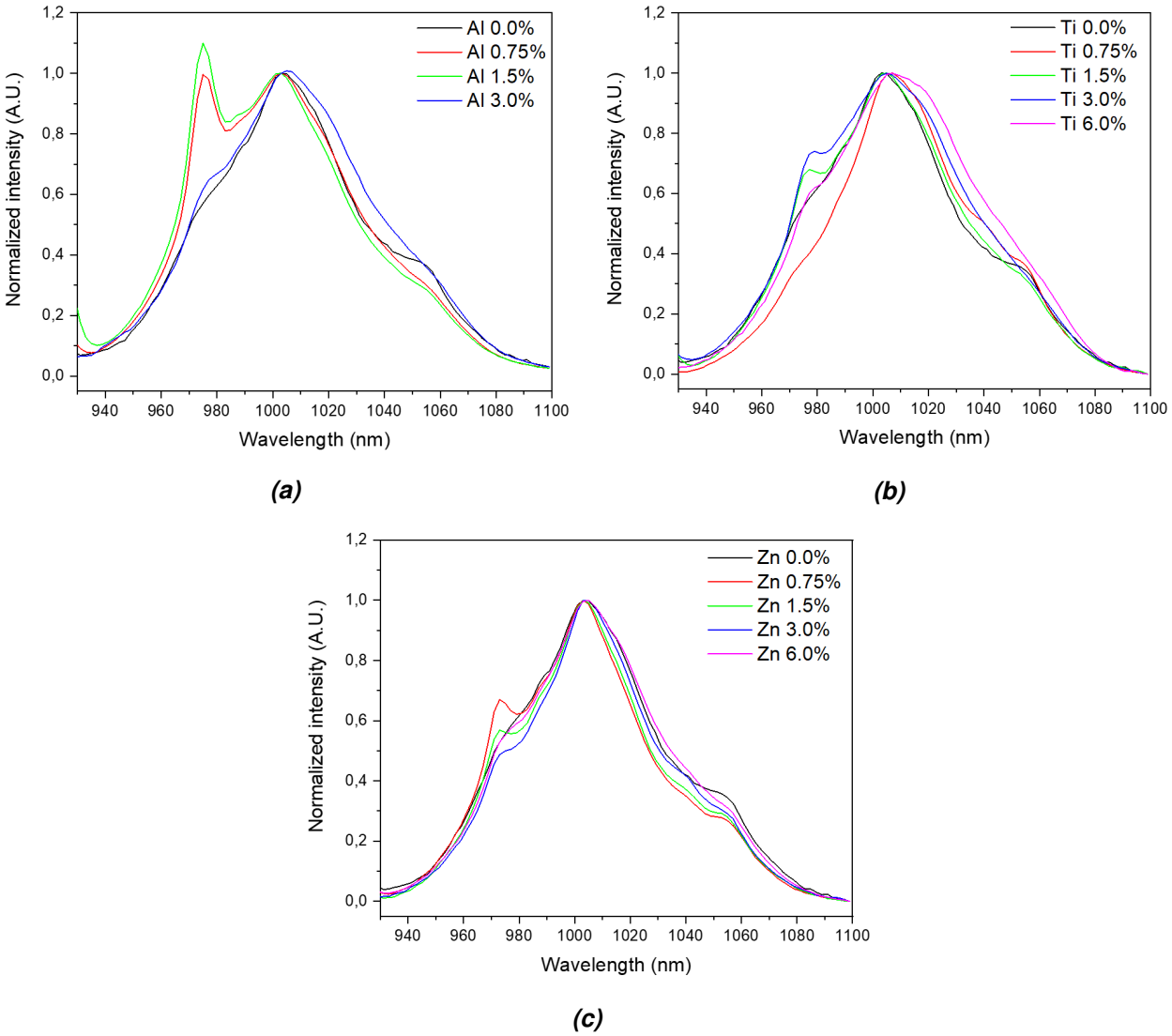

Figure 4.6. *Normalized emission spectra of the heat-treated glasses with 900 nm excitation.*

The heat-treated Al-glass shows an increase in the relative intensity of emission at around 975 nm and a decrease at around 1060 nm, with increasing concentrations of Al_2O_3. Similar effect can be seen on the Ti- and Zn-glasses but to a lesser extent. This shows that the added oxides modify the luminescence properties of the heat-treated glasses. The energy levels of the Yb^{3+}-ion in the crystal phase of $NaYb(P_2O_7)$ are very sensitive to changes in the coordination sphere of the Yb^{3+}-ion, and change through Stark splitting [24] [37]. Because of this, it is most likely that the added oxides modify the coordination sphere of the Yb^{3+}-ion and cause the emission lines to shift from 1060 nm, to 1005 nm and 975 nm.

5 CONCLUSION

The thermal, optical and luminescence properties, and the hygroscopicity of glasses in the system (98.75 - x) mol % [90 $NaPO_3$ – 10 Na_2O] – x mol% [Al_2O_3, TiO_2, or ZnO] – 1.25 mol% [Yb_2O_3] were studied. The glasses were prepared with a standard melt quench method. The Al- and Ti-glasses showed an increase in their thermal properties, which indicates that they modify the phosphate glass network by creating new P-O-Al/Ti -bonds at the expense of the normal P-O-P -bonds. The Zn-glass did not appear to modify the glass network and it is expected to enter the glass as a network modifier. All the prepared glasses showed an increase on their optical properties, which include the absorption coefficient and the absorption cross-section. This is an indication that all the added oxides modified the coordination sphere of the optically active ion of Yb^{3+}. Also, the intensities of emission and the emission cross-sections at 975 nm increased. In FTIR measurements the glasses showed a decrease in the intensity of the absorption at 2800 cm^{-1} which is related with strongly associated OH- groups in the glass structure. This implies that all the glasses were more water resistant and less hygroscopic with the addition of the oxides.

The glasses were also heat treated at T_g + 20 ℃ for 17 hours and then at T_p for two hours to turn them into glass-ceramics. The crystalline structure of the glasses was measured with an XRD. Two crystalline phases were identified $NaYb(P_2O_7)$ and $Na_5(P_3O_{10})$, of which the first one is considered a good crystalline phase for optical applications, like fiber lasers. The emission spectra of the heat-treated glasses were also measured. The addition of the oxides appears to shift the emission band form 1060 nm, to 975 nm and 1005 nm probably because of Stark splitting of the optically active ion of Yb^{3+}.

For the next steps, the heat treatment parameters, which are time and temperature, should be further optimized to create transparent glass ceramics with higher concentrations of the $NaYb(P_2O_7)$ crystalline phases, or other phases which contain the optically active ion of Yb^{3+}. Also, it would be preferable to create glass ceramics with more bulk crystals and less surface crystals. Additionally, the effects of other metal oxides like MgO or Li_2O on similar oxyphosphate glasses should be further studied.

REFERENCES

[1] Bretenaker, F. and Treps, N. *Laser: 50 Years Of Discoveries.* World Scientific, 2014, pp. 1, 86–87. ISBN: 9789814612401.

[2] DiGiovanni, D., Shubochkin, R., Morse, T. and Lenardic, B. *Rare Earth-Doped Fibers, in: A. Mendez and T. Morse (ed.), Specialty Optical Fibers Handbook*. Elsevier Science Technology, 2007, pp. 198–200. ISBN: 9780080474991.

[3] Jones, J. and Clare, A. *Bio-glasses : an introduction*. John Wiley & Sons, Incorporated, 2012, pp. 45–63. ISBN: 978-0-470-71161-3.

[4] Hongisto, M., Veber, A., Boetti, N., Danto, S., Jubera, V. and Petit, L. Transparent Yb3+ doped phosphate glass-ceramics. *Ceramics International* Vol. 46.No. 16, Part B (2020), pp. 26317–26325. ISSN: 0272-8842. DOI: 10.1016/j.ceramint.2020.01.121.

[5] Semenov, V., Cherepennikova, N., Grigor'ev, I., Klapshina, L., Kuznetsova, O., Lopatin, M., Bushuk, B., Bushuk, S., Kal'vinkovskaya, Y. and Douglas, W. Europium, terbium, and ytterbium 3-(3-triethoxysilylpropyl)pentane-2,4-dionates. Synthesis and the formation of luminescent sol-gel films. *Russian Journal of Coordination Chemistry* Vol. 33.No. 1 (2007), pp. 68–78. DOI: 10.1134/S1070328407010101.

[6] Henderson, J. *Ancient Glass : An Interdisciplinary Exploration*. Cambridge University Press, 2013, pp. 8–12. ISBN: 9781139021883.

[7] Zhang, C., Wang, L., Ji, X., Li, G. and Hou, G. Effect of Melting Times on the Down-Shifting Properties in Ce3+-Doped Oxyfluoride Glass Ceramics for a-Si Solar Cells. *Journal of Russian Laser Research* Vol. 38.No. 6 (2017), pp. 554–558. DOI: 10.1007/s10946-017-9679-8.

[8] Shelby, J. *Introduction to glass science and technology*. The Royal Society of Chemistry, 2005, pp. 4, 26–30. ISBN: 978-0-85404-639-3.

[9] Le Bourhis, E. *Glass : mechanics and technology*. John Wiley & Sons, Incorporated, 2014, pp. 85–88. ISBN: 978-3-527-67944-7.

[10] Garcia-Valles, M., Hafez, H., Cruz-Matías, I., Vergés, E., Aly, M., Nogués, J., Ayala, D. and Martínez, S. Calculation of viscosity–temperature curves for glass obtained from four wastewater treatment plants in Egypt. *Journal of Thermal Analysis and Calorimetry* Vol. 111.No. 1 (2013), pp. 107–114. ISSN: 1572-8943. DOI: 10.1007/s10973-012-2232-7.

[11] Varshneya, A. and Mauro, J. *Fundamentals of Inorganic Glasses*. Elsevier, 2019, pp. 1–18, 50–61. ISBN: 978-0-12-816225-5.

[12] Zachariasen, W. The atomic arrangement in glass. *Journal of the American Chemical Society* Vol. 54.No. 10 (1932), pp. 3841–3851. DOI: 10.1021/ja01349a006.

[13] Johnson, W. Bulk amorphous metal–an emerging engineering material. *JOM* Vol. 54.No. 3 (2002), pp. 40–44. ISSN: 10474838.

[14] Masayuki, Y. and Yoshiyuki, A. *Glasses for photonics*. Cambridge University Press, 2004, p. 3. ISBN: 9780511541308.

[15] Robertson, J. Silicon versus the rest. *Canadian Journal of Physics* Vol. 92.No. 7 (2014), pp. 553–560.

[16] Fu, A. and Mauro, J. Topology of alkali phosphate glass networks. *Journal of Non-Crystalline Solids* Vol. 361 (2013), pp. 57–62. ISSN: 0022-3093. DOI: 10.1016/j.jnoncrysol.2012.11.001.

[17] Nian, S., Zhang, Y., Li, J., Zhou, N. and Zou, W. Glass formation and properties of sodium zinc phosphate glasses doped with ferric oxide. *Advances in Applied Ceramics: Structural, Functional Bioceramics* Vol. 117.No. 6 (2018), pp. 319–327. ISSN: 17436753.

[18] Bunker, B., Arnold, G. and Wilder, J. Phosphate glass dissolution in aqueous solutions. *Journal of Non-Crystalline Solids* Vol. 64.No. 3 (1984), pp. 291–316. ISSN: 0022-3093. DOI: 10.1016/0022-3093(84)90184-4.

[19] Bünzli, J.-C. New exciting challenges in lanthanoid photonics: telecommunications and solar energy conversion, in: Z. Liu (ed.), Rare-earths new research. (2013), pp. 1–12.

[20] Doosti, A., Keshavarzi, A., Yazd, N. and Leriche, A. Laser-induced and space-selective crystallization of yttrium aluminum garnet crystal from SiO2/Al2O3/Y2O3 /KF/Na2O/AlF3/B2O3 glass system. *CrystEngComm* Vol. 23.No. 5 (2021), pp. 1110–1116. DOI: 10.1039/D0CE01165G.

[21] Ohkawa, H., Hayashi, H. and Kondo, Y. Influence of water on non-radiative decay of Yb3+ - 2F5/2 level in phosphate glass. *Optical Materials* Vol. 33 (2010), pp. 128–130.

[22] Meshkova, S., Topilova, Z., Devyatykh, N., Gusev, A. and Shul'gin, V. IR luminescence of neodymium(III) and ytterbium(III) ions in complexes with N-alkyl-substituted 2-aminobenzoic acids. *Russian Journal of Inorganic Chemistry* Vol. 56.No. 2 (2011), pp. 262–266.

[23] Mathieu, A. and Laurent, C. *Crystallization and Glass-Ceramics, in: D. Musgraves and J. Hu and L. Calvez (ed.) Springer Handbook of Glass*. Springer International Publishing, 2019, pp. 113–167. ISBN: 978-3-319-93728-1. DOI: 10.1007/978-3-319-93728-1_4.

[24] Ternane, R., Ferid, M., Guyot, Y., Trabelsi-Ayadi, M. and Boulon, G. Spectroscopic properties of Yb3+ in NaYbP2O7 diphosphate single crystals. *Journal of Alloys and Compounds* Vol. 464.No. 1–2 (2008), pp. 327–331. ISSN: 0925-8388. DOI: 10.1016/j.jallcom.2007.09.104.

[25] Ghandi, K. A Review of Ionic Liquids, Their Limits and Applications. *Green and Sustainable Chemistry* Vol. 4 (2014), pp. 44–53.

[26] Özen, G., Aydinli, A., Cenk, S. and Sennaroğlu, A. Effect of composition on the spontaneous emission probabilities, stimulated emission cross-sections and local environment of Tm3+ in TeO2–WO3 glass. *Journal of Luminescence* Vol. 101.No. 4 (2003), pp. 293–306. ISSN: 0022-2313. DOI: 10.1016/S0022-2313(02)00572-0.

[27] Jiang, C., Deng, P., Zhang, J., Huang, G. and Gan, F. Yb:tellurogermanate laser glass with high emission cross section. *Journal of Luminescence* Vol. 82.No. 4 (1999), pp. 321–326. ISSN: 0022-2313. DOI: 10.1016/S0022-2313(99)00049-6.

[28] Larkin, P. *Infrared and Raman Spectroscopy*. Elsevier, 2011, p. 31. ISBN: 978-0-12-386984-5.

[29] Suryanarayana, C. *Experimental techniques in materials and mechanics*. Taylor & Francis Group, 2011, p. 43. ISBN: 0-429-10920-2.

[30] Voronko, Y., Lomonova, E., Osiko, V., Sobol, A., Ushakov, S. and Shukshin, V. Active laser media based on fianite crystals. *Quantum Electronics* Vol. 36.No. 7 (2006), pp. 601–608. DOI: 10.1070/qe2006v036n07abeh013185.

[31] Metwalli, E. and Brow, R. Modifier effects on the properties and structures of aluminophosphate glasses. *Journal of Non-Crystalline Solids* Vol. 289.No. 1 (2001), pp. 113–122. ISSN: 0022-3093. DOI: 10.1016/S0022-3093(01)00704-9.

[32] Kundu, R., Dhankhar, S., Punia, R., Sharma, S. and Kishore, N. ZnCl2 Modified Physical and Optical Properties of Barium Tellurite Glasses. *Transactions of the Indian Ceramic Society* Vol. 72.No. 3 (2013), pp. 206–210. DOI: 10.1080/0371750X.2013.851883.

[33] Tiwari, B., Sudarsan, V., Dixit, A. and Kothiyal, G. Effect of TiO2 Addition on the Optical, Thermo-Physical, and Structural Aspects of Sodium Alumino-Phosphate Glasses. *Journal of the American Ceramic Society* Vol. 94.No. 5 (2011), pp. 1440–1446. DOI: 10.1111/j.1551-2916.2010.04292.x.

[34] Hyppänen, I., Hölsä, J., Kankare, J., Lastusaari, M., Pihlgren, L. and Soukka, T. Defect Structure and Up-conversion Luminescence Properties of ZrO2:Yb3+,Er3+ Nanomaterials. *Journal of Fluorescence* Vol. 18 (2008), pp. 1029–1034. DOI: 10.1007/s10895-008-0327-0.

[35] Efimov, A., Pogareva, V. and Shashkin, A. Water-related bands in the IR absorption spectra of silicate glasses. *Journal of Non-Crystalline Solids* Vol. 332.No. 1 (2003), pp. 93–114. ISSN: 0022-3093. DOI: 10.1016/j.jnoncrysol.2003.09020.

[36] Navarra, G., Iliopoulos, I., Militello, V., Rotolo, S. and Leone, M. OH-related infrared absorption bands in oxide glasses. *Journal of Non-Crystalline Solids* Vol. 351.No. 21 (2005), pp. 1796–1800. ISSN: 0022-3093. DOI: 10.1038/s41598-020-73341-4.

[37] Zhang, L., Hu, L. and Jiang, S. Progress in Nd3+, Er3+, and Yb3+ doped laser glasses at Shanghai Institute of Optics and Fine Mechanics. *International Journal of Applied Glass Science* Vol. 9 (2018), pp. 90–98. DOI: 10.1111/ijag.12283.